RESEARCH PAPER

Dose and Time-Dependent Hepatic and Renal Toxicity of Arsenic Exposure in Rats- A Qualitative Histopathological Study

Sauliha Rafiq [1], Mahak Mushtaq[1], Munibul Rehman[1], Ghulam M Bhat[2], Rohi Wani[3]
[1,2]Department of Anatomy, Government Medical College Srinagar, J&K, India.
[3]Department of Pathology, Government Medical College Srinagar, J&K, India
Corresponding Author
Dr. Ghulam Mohammad Bhat,
Professor of Anatomy, Government Medical College Srinagar, 190001, J&K, India
Email: gmbhat144@gmail.com

ABSTRACT
Background: Arsenic is a well-recognized environmental toxin with cumulative effects on multiple organs, particularly the liver and kidneys. Experimental models provide valuable insights into the dose- and time-dependent progression of arsenic-induced toxicity.
Objective: To evaluate the gross and microscopic changes in the liver and kidneys of rats following chronic exposure to arsenic at two different dose levels over 4, 8, and 12 weeks.
Methods: Adult rats were divided into three groups: controls (Group A), low-dose arsenic exposure (50 ppm; Group B), and high-dose arsenic exposure (100 ppm; Group C). Animals were sacrificed at 4, 8, and 12 weeks, and liver and kidney tissues were examined grossly and microscopically.
Results: In the Arsenic treated rats, the liver developed focal inflammatory infiltrates and venous congestion at 4–8 weeks, progressing to central and portal venous dilatation with congestion by 12 weeks. As the study advanced, there was central vein degeneration, neutrophilic infiltration, and ballooning degeneration of hepatocytes, accompanied by nodularity and discoloration. In the kidney, there was widening of Bowman's space and glomerular hypercellularity with tubular vacuolization by 12 weeks. Later on, there were more severe changes, including interstitial hemorrhage and vascular congestion at 4 weeks, glomerular shrinkage and marked Bowman's space expansion at 8 weeks, and extensive interstitial hemorrhage, tubular necrosis, and fibrosis with enlargement and hemorrhagic patches.
Conclusion: Chronic arsenic exposure produces progressive, dose- and time-dependent hepatic and renal injury. Early microscopic changes like vascular congestion, glomerular alterations, and inflammatory infiltrates precede organ alterations such as enlargement, nodularity, and hemorrhage.
Keywords Arsenic toxicity, Hepatotoxicity, Nephrotoxicity, Histopathology, Tubular necrosis
How to cite this article: Rafiq S, Mushtaq M, Rehman M, Bhat GM, Wani R. Dose and Time-Dependent Hepatic and Renal Toxicity of Arsenic Exposure in Rats - A Qualitative Histopathological Study. Int J Drug Deliv Technol. 2026;16(51s): 858-865. DOI: 10.25258/ijddt.16.51s.70

Source of support: Nil.
Conflict of interest: Nil.

INTRODUCTION

Arsenic is a naturally occurring metalloid with well-recognized toxic and carcinogenic potential. Widespread contamination of groundwater in regions of South and Southeast Asia, as well as parts of South America, has made arsenic exposure a major global public health problem.[1,2] Chronic arsenic ingestion, primarily in the form of inorganic salts such as sodium arsenate, has been linked to a broad spectrum of clinical outcomes ranging from dermatologic changes and neuropathy to cardiovascular disease and malignancy.[3] Importantly, arsenic has a pronounced tropism for visceral organs, particularly the liver and kidneys, which serve as central sites of xenobiotic metabolism, detoxification, and excretion.

The liver is the primary organ responsible for arsenic biotransformation. In hepatocytes, arsenic undergoes reduction and oxidative methylation, processes that generate reactive oxygen species (ROS) and disrupt antioxidant defense systems.[4,5] These mechanisms can initiate a cascade of cellular injury including oxidative stress, mitochondrial dysfunction, impaired energy metabolism, and cell death.[5] Histopathological hallmarks reported in animal and human studies include hepatocellular necrosis, sinusoidal dilatation, portal tract inflammation, and in severe or prolonged exposure, fibrosis and cirrhosis.[6,7] Beyond the liver, the kidneys represent a second critical target. Renal proximal tubular cells are directly exposed to filtered arsenic metabolites and are highly susceptible to oxidative and inflammatory damage. Histological features of arsenic nephrotoxicity include glomerular hypercellularity, tubular vacuolization, necrosis, interstitial inflammation, and, with chronicity, fibrosis.[8-10]

Although arsenic toxicity is well established, important knowledge gaps remain regarding the dose time relationship of hepatic and renal injury under controlled experimental conditions. Many prior investigations have

*Author for Correspondence: Dr. Ghulam Mohammad Bhat,

used acute high-dose exposure models that may not reflect the subtler, progressive injury seen with environmentally relevant chronic exposure.[11,12] Moreover, detailed comparative histopathological studies that examine both liver and kidney across multiple durations and dose levels remain limited. Such systematic evaluation is critical not only for clarifying organ-specific vulnerability but also for providing translational insights into the pathology of human arsenicosis, where clinical findings often evolve insidiously over years.

Animal models, particularly Wistar rats, offer a robust platform to address these gaps. Their well-characterized physiology, reproducible histological responses, and sensitivity to oxidative and toxic insults make them suitable for dissecting the pathogenesis of arsenic injury. By examining organ morphology at defined timepoints, experimental studies can delineate the trajectory of lesion development, identify early markers of toxicity, and evaluate dose-dependency. In this context, the present study was designed to investigate the hepatic and renal histopathological alterations induced by chronic sodium arsenate exposure in male Wistar rats. Animals were administered arsenic at two dose levels (50 ppm and 100 ppm) over 4, 8, and 12 weeks, and their livers and kidneys were examined for changes. This approach provides an opportunity to map the progression of lesions in a structured time-dependent manner and to compare the severity of effects across doses. By doing so, the study aims to contribute to a more nuanced understanding of arsenic hepatotoxicity and nephrotoxicity, with emphasis on the morphologic correlates of cumulative exposure.

Material and methods

The present experimental study was carried out in the Postgraduate Department of Anatomy in collaboration with the Department of Pathology, Government Medical College, Srinagar, over a period of 18 months, including one year for data collection and six months for compilation and analysis. Ethical clearance for the use of experimental animals was obtained from the Institutional Animal Ethics Committee (IAEC/Pharma/MC/19), and all procedures were conducted in accordance with the guidelines of the Committee for the Purpose of Control and Supervision of Experiments on Animals (CPCSEA).

A total of eighteen healthy adult male Wistar albino rats, weighing between 180 and 250 g, were procured from the Central Animal House of Government Medical College, Srinagar. Minimum number of animals were used as per the recommendations of the Institutional Animal Ethics Committee. Only apparently healthy animals were included, while those that were underweight, lethargic, feeding poorly, showing weight loss, diarrhoea, generalized hair loss, or other signs of ill-health were excluded. Prior to the experiment, all animals were acclimatized for one week under standard laboratory conditions, housed in polypropylene cages (44 × 28.6 × 30 cm^3) with dust-free husk bedding in a well-ventilated room maintained at a temperature of 18–29°C, relative humidity of 30–70%, and a 12-hour light/dark cycle. Standard rodent chow and tap water were provided ad libitum, and the principles of reduction, refinement, and replacement were carefully observed.

The animals were randomized into three groups of six rats each. Group A served as untreated controls and received only standard diet and tap water. Group B received sodium arsenate at a concentration of 50 ppm (50 mg/L) in drinking water in addition to the standard diet, while Group C received sodium arsenate at 100 ppm (100 mg/L). Sodium arsenate heptahydrate was obtained from Oxford Lab Fine Chem LLP Vasai, Dist. Palghar. Sodium arsenate solutions were freshly prepared before administration by dissolving the required amount of sodium arsenate in one Liter of tap water to ensure stability and consistent dosing. All animals were observed daily for physical activity, feeding patterns, and any abnormal clinical signs.

At predetermined intervals of 4, 8, and 12 weeks, animals were anesthetized with chloroform inhalation and sacrificed as per CPCSEA guidelines. A systematic external examination was performed to note body condition, skin status, and the presence of external lesions or discharges. The animals were laid supine on a dissection tray, disinfected with 70% ethanol, and subjected to a midline abdominal incision to expose the thoracoabdominal viscera. Gross examination of the liver and kidneys was performed in situ to record organ size, colour, and surface morphology. Both organs were then carefully dissected, rinsed in normal saline, and fixed in 10% neutral buffered formalin for further processing.

Histological examination was performed following standard manual techniques. Tissues were cut into 5 mm slices, fixed for 7–10 days in 10% formalin, and processed through graded alcohols for dehydration, xylene for clearing, and paraffin wax for embedding at 58–60°C. Paraffin blocks were sectioned at 6–8 µm thickness using a rotary microtome, and sections were mounted on albumin-coated glass slides. Slides were stained with Hematoxylin and eosin using Harris's method for nuclear and cytoplasmic detail, dehydrated through ascending grades of alcohol, cleared in xylene, and mounted with DPX. Stained sections were examined under a light microscope, and photomicrographs were taken for documentation. Changes were recorded systematically for each group at each timepoint, with specific attention to hepatocellular degeneration, vascular congestion, necrosis, inflammatory infiltrates, and glomerular or tubular alterations in the kidney. Histopathological evaluation was performed by a pathologist blinded to group allocation. A single pathologist examined the slides for interpretation of the microscopic changes.

Results

Gross Findings of liver and kidney

In control animals (Group A), the liver appeared normal at all timepoints, maintaining a smooth surface with preserved size, shape, and colour. Group B animals showed no visible alterations at 4 and 8 weeks, but by 12 weeks, the liver appeared slightly enlarged. In Group C, gross hepatic changes were more pronounced at 12 weeks, with surface nodularity and discoloration becoming evident, reflecting the severity of arsenic-induced injury. The kidneys of

control rats (Group A) remained normal in gross appearance throughout the study. Group B kidneys were grossly unremarkable at 4 and 8 weeks but demonstrated enlargement with haemorrhagic spots by the 12th week. In Group C, kidneys initially appeared normal at 4 and 8 weeks, but by 12 weeks, they showed severe enlargement, irregular surfaces, and prominent haemorrhagic patches, suggesting more advanced damage compared to Group B.

Microscopic Findings of liver

In Group A, microscopic examination consistently revealed normal hepatic architecture across all timepoints. Well-organized hexagonal lobules were observed with central veins at the core, radiating hepatic cords, and intact portal triads composed of the portal vein, hepatic arteriole, and bile duct, all surrounded by connective tissue.

Table 1. Showing Liver Findings Across Groups and Timepoints (Figure 1- A, B, C, and D)

Timepoint	Group A (Control)	Group B (50 ppm)	Group C (100 ppm)
4 weeks	Gross: Normal size, shape, and color. Histology: Preserved lobular architecture with central vein, hepatic cords, and intact portal triads.	Gross: Normal. Histology: Focal inflammatory cell aggregates.	Gross: Normal. Histology: Central vein degeneration and congestion.
8 weeks	Gross: Normal. Histology: Normal lobular architecture.	Gross: Normal. Histology: Neutrophilic infiltration and central venous congestion.	Gross: Normal. Histology: Neutrophilic infiltration with central venous dilatation and degeneration.
12 weeks	Gross: Normal. Histology: Preserved architecture.	Gross: Slightly enlarged liver. Histology: Central and portal venous dilatation with congestion.	Gross: Surface nodularity and discoloration. Histology: Portal venous dilatation with congestion, chronic inflammatory infiltrates, ballooning degeneration of hepatocytes.

At 4 weeks, Group B livers showed focal inflammatory cell aggregates, while Group C demonstrated focal degeneration and congestion in the central veins. By 8 weeks, Group B exhibited neutrophilic infiltration with central venous congestion, whereas Group C showed more severe lesions, including neutrophilic infiltration, central venous dilatation, and degeneration. At 12 weeks, Group B displayed central and portal venous dilatation accompanied by congestion, while Group C demonstrated advanced pathological changes, including portal venous dilatation with congestion, chronic inflammatory cell infiltrates, and ballooning degeneration of hepatocytes. These findings indicate a clear time- and dose-dependent progression of hepatic injury, with Group C consistently showing more pronounced alterations than Group B.

Microscopic Findings of kidney

Microscopic evaluation of control kidneys (Group A) confirmed normal renal architecture at all timepoints, characterized by well-preserved glomeruli, intact Bowman's capsules, and organized renal tubules.

Table 2: Kidney Findings Across Groups and Timepoints (Figure 2- A, B, C, and D)

Timepoint	Group A (Control)	Group B (50 ppm)	Group C (100 ppm)
4 weeks	Gross: Normal size, color, texture. Histology: Preserved renal architecture.	Gross: Normal. Histology: Normal.	Gross: Normal. Histology: Interstitial hemorrhage and vascular congestion.
8 weeks	Gross: Normal. Histology: Normal renal architecture.	Gross: Normal. Histology: Widened Bowman's space.	Gross: Normal. Histology: Glomerular tuft shrinkage and marked increase in Bowman's space.
12 weeks	Gross: Normal. Histology: Preserved renal architecture.	Gross: Enlarged with hemorrhagic spots. Histology: Increased Bowman's space, glomerular hypercellularity, tubular epithelial vacuolization.	Gross: Severely enlarged with irregular surface and prominent hemorrhages. Histology: Extensive interstitial hemorrhage, tubular necrosis, interstitial fibrosis.

At 4 weeks, no histological changes were noted in Group B kidneys, while Group C exhibited early vascular alterations, including interstitial hemorrhage and vascular congestion. By 8 weeks, Group B showed widening of Bowman's space, whereas Group C demonstrated glomerular tuft shrinkage accompanied by a marked increase in Bowman's space. At 12 weeks, Group B kidneys exhibited enlargement with hemorrhagic spots, hypercellularity of glomeruli, and vacuolization of tubular epithelium in addition to widening of Bowman's space. In Group C, the renal pathology was more severe, characterized by gross enlargement and irregular surface features on gross

examination, and microscopically by extensive interstitial hemorrhage, tubular necrosis, and interstitial fibrosis.

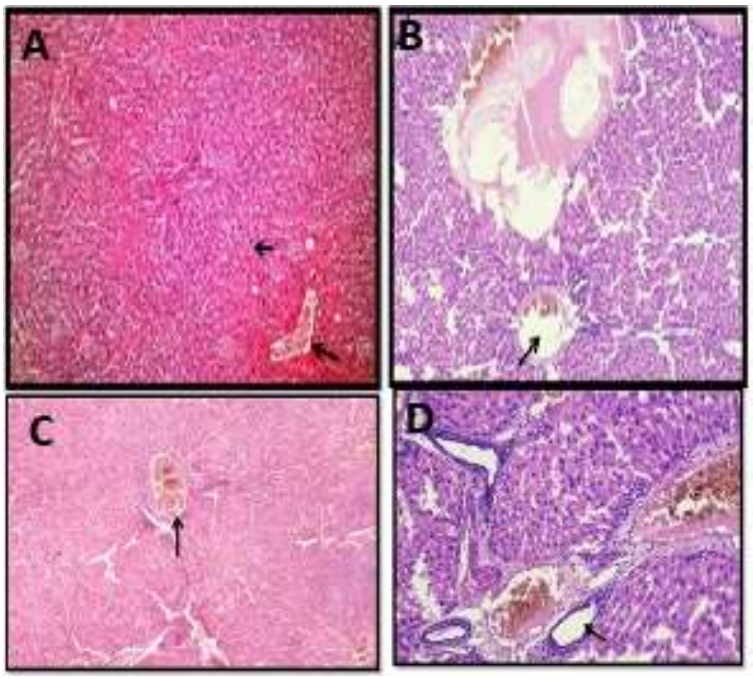

Figure 1
Microphotograph of the liver from Group A at the end of 4 Weeks showing normal hepatic cords and central vein in liver histology. (Stain: H&E Magnification: 40x).
Microphotograph of the liver from Group B at the end of 12 Weeks showing central venous and portal vein dilation and congestion. (Stain: H&E Magnification: 40x)
Microphotograph of the liver from Group C at the end of 4 Weeks showing foci of central vein degeneration and congestion. (Stain: H&E Magnification: 40x)
Microphotograph of the liver from Group C at the end of 12 Weeks showing Liver portal venous dilation and congestion with chronic inflammatory cell infiltrates and ballooning degeneration of hepatocytes. (Stain: H&E Magnification: 100x)

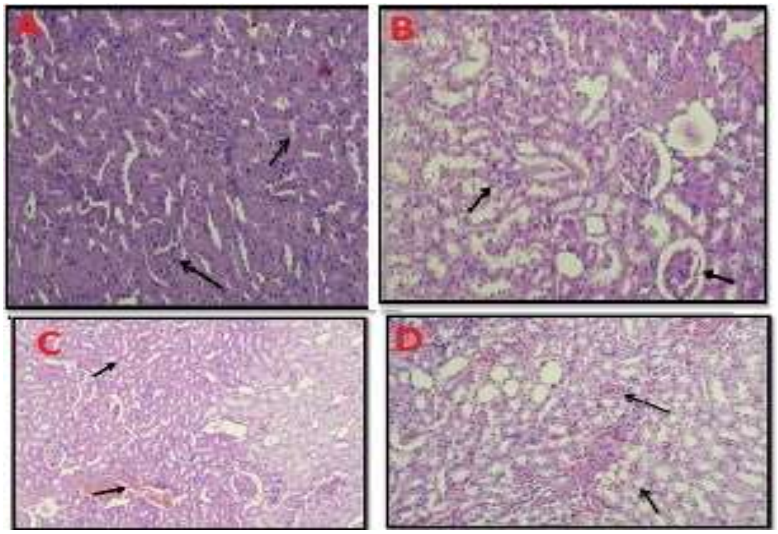

Figure 2
Microphotograph of the Kidney from Group A at the end of 4 Weeks showing normal glomerulus and tubular histology. (Stain: H&E Magnification: 40x)

Microphotograph of the Kidney from Group B at the end of 12 Weeks showing increase in bowman's space. Hyper-cellularity of glomeruli, vacuolization of tubular epithelium. (Stain: H&E Magnification: 40x)
Microphotograph of the Kidney from Group C at the end of 4 Weeks Showing Interstitial haemorrhage and vascular congestion. (Stain: H&E Magnification: 100x)
Microphotograph of the Kidney from Group C at the end of 12 Weeks showing extensive interstitial haemorrhage (Stain: H&E Magnification: 40x)

Discussion

In the present study, the gross morphology of the liver and kidney revealed a clear dose- and time-dependent trajectory of arsenic toxicity. Control animals consistently maintained normal organ appearance, confirming the absence of spontaneous pathology and establishing a reliable baseline. In exposed groups, no visible changes were noted at 4 or 8 weeks, which is in line with reports that early arsenic-induced injury is largely microscopic and biochemical in nature, preceding overt macroscopic manifestations. By 12 weeks, Group B animals showed only mild hepatic enlargement, whereas Group C animals exhibited more conspicuous gross abnormalities, including surface nodularity and discoloration. Such features are consistent with previous studies demonstrating that subchronic arsenic exposure induces hepatomegaly, congestion, and fibrotic remodeling, which eventually manifest as irregular surfaces and color changes of the liver.[13,14] Experimental models have linked these macroscopic changes to progressive oxidative stress, periportal inflammation, and collagen deposition in the liver parenchyma, which initially develop microscopically before becoming grossly evident at higher doses and longer exposures. For instance, Santra *et al.* (2000) observed in chronically arsenic-dosed mice that significant oxidative stress preceded fibrotic changes; early reductions in hepatic glutathione and antioxidant enzyme activity occurred before any gross hepatic abnormalities became apparent, with hepatic fibrosis manifesting only after months of exposure.[15] Ramadan *et al.* (2024) further confirmed that arsenic exposure led to increased collagen deposition in both central and portal regions of rat livers, mediated by oxidative stress pathways and inflammatory signaling.[13] These findings are in strong agreement with our data, which show early microscopic liver injury followed by gross morphologic change in a dose- and time-dependent manner. A parallel trend was observed in the kidney. Controls remained grossly normal throughout the study, while Group B kidneys were unaffected at 4 and 8 weeks but became enlarged with haemorrhagic spots by 12 weeks. In contrast, Group C showed severe renal enlargement, irregular surfaces, and prominent cortical haemorrhages at the same timepoint, reflecting more advanced vascular and tubular injury. These findings agree with established literature identifying the kidney as a critical target of arsenic toxicity, where interstitial haemorrhage, vascular congestion, and tubular necrosis are common features.[16] Studies in arsenic-exposed rodents have similarly reported renal enlargement and mottled haemorrhagic appearances after subchronic dosing, confirming the consistency of our observations with experimental models.[17,18]The time lag between early histological lesions and later gross organ changes in our study is particularly noteworthy. Toxicologic pathology guidelines and prior experimental studies emphasize that gross morphology often underrepresents the true extent of injury, with macroscopic alterations becoming apparent only after cumulative structural damage surpasses a threshold. Our results mirror this principle, as microscopic injury was detectable as early as 4 weeks, whereas gross changes emerged only by 12 weeks in the exposed groups, especially at the higher dose.

The present study demonstrated a clear, time- and dose-dependent progression of microscopic hepatic alterations following arsenic exposure, with Group A (controls) consistently maintaining normal histoarchitecture at all timepoints. Well-organized hexagonal lobules, intact central veins, and clearly defined portal triads were observed in controls, confirming the absence of spontaneous lesions and validating the observed changes in arsenic-exposed groups as exposure-related effects. By 4 weeks, Group B livers revealed focal aggregates of inflammatory cells, while Group C showed focal degeneration and congestion in the central veins. These early microscopic lesions are consistent with prior experimental models of arsenic hepatotoxicity, where low-dose or short-term exposure produces venous congestion and mild inflammatory infiltration as the first signs of liver injury (Shangloo et ., 2021).[19] Such lesions are often attributed to oxidative stress-induced endothelial dysfunction and low-grade inflammatory activation, which precede more advanced parenchymal injury as also reported by Ibrahim et al.[20] At 8 weeks, arsenic-related damage became more pronounced. Group B displayed neutrophilic infiltration and central venous congestion, whereas Group C developed more severe lesions, including central venous dilatation, neutrophilic infiltration, and hepatocellular degeneration. These findings are consistent with experimental studies conducted by Ghatak et. al and Wen et. al. who described progressive vascular congestion and inflammatory cell recruitment as intermediate steps in arsenic hepatotoxicity, which later evolve into necrotic inflammatory changes and hepatocyte injury.[22,23] The presence of hepatocellular degeneration in Group C underscores the higher vulnerability of hepatic parenchyma at greater exposure levels.

By 12 weeks, the distinction between dose groups became even clearer. Group B livers showed central and portal venous dilatation with congestion, while Group C developed advanced lesions, including portal venous dilatation, chronic inflammatory infiltrates, and ballooning degeneration of hepatocytes. These observations are strongly supported by prior experimental work. Ramadan *et al.* reported that arsenic-treated rats developed marked central venous dilatation and portal-tract congestion,

paralleling the vascular changes we observed in Group B at 12 weeks.[13] Similarly, Shangloo *et al.* demonstrated that chronic arsenic exposure in mice led to periportal inflammation and vascular congestion, which preceded hepatocellular degeneration and fibrosis, aligning closely with the stepwise lesions in our study.[19]Group C's more advanced microscopic pattern with portal venous dilatation with congestion, chronic inflammatory infiltrates, and ballooning degeneration of hepatocytes is likewise consistent with the literature describing arsenic's time and dose-dependent transition from inflammatory vascular lesions to frank degenerative remodelling. Ghatak et al. demonstrated that oxidative stress triggered by arsenic exposure activates hepatic stellate cells, which in turn drive hepatocellular ballooning and subsequent fibrotic remodelling in mice.[22] This suggests that ballooning is a pivotal histological marker, signifying the transition from an inflammatory stage to a fibrogenic response. Likewise, Li *et al.* observed hepatocyte ballooning and hydropic degeneration in arsenic-exposed rodents, describing these lesions as precursors to fibrosis and cirrhosis.[24] The concurrence of our findings with these established models underscores that ballooning degeneration reflects not only direct oxidative injury to hepatocytes but also the initiation of irreversible structural remodelling of the liver.

The microscopic evaluation of kidneys in control animals (Group A) consistently demonstrated well-preserved glomeruli, intact Bowman's capsules, and organized renal tubules at all timepoints, reflecting normal renal architecture and confirming the absence of spontaneous lesions. These findings provided a reliable baseline against which arsenic-induced changes in the exposed groups could be compared. By four weeks, no histological alterations were evident in Group B, whereas Group C already displayed early vascular lesions, including interstitial haemorrhage and vascular congestion. Similar early vascular disturbances have been described in rodent arsenic models, where peritubular congestion and interstitial haemorrhagic foci appear as initial signs of renal injury (Ferzand *et al.*, 2008).[26] These changes suggest that vascular dysfunction is one of the earliest renal responses to arsenic toxicity. At eight weeks, lesions became more distinct. Group B developed widening of Bowman's space, while Group C exhibited glomerular tuft shrinkage accompanied by a marked expansion of Bowman's space. This pattern is consistent with the observations of Roy and Bhattacharya, who reported glomerular shrinkage and Bowman's space dilation in arsenic-exposed fish kidneys, indicating that glomerular collapse and filtration barrier compromise are common outcomes of chronic arsenic exposure.[27]

By twelve weeks, the pathological changes were more advanced and dose-dependent. Group B kidneys showed enlargement with hemorrhagic spots, hypercellularity of glomeruli, and vacuolization of tubular epithelium in addition to Bowman's space widening. In Group C, renal injury was more severe, with gross enlargement and irregular surfaces accompanied microscopically by extensive interstitial hemorrhage, tubular necrosis, and fibrosis. Such advanced lesions closely mirror those reported by Ferzand et al in chronic arsenic exposure studies in rodents, where tubular degeneration, necrosis, and interstitial scarring are hallmark findings after sustained exposure.[26] These advanced lesions mirror the chronic nephrotoxicity described in multiple experimental studies. Gupte et al. reported that rats exposed to low-dose arsenic exhibited glomerular shrinkage, widened periglomerular space, and vascular congestion changes that were also evident in our Group B at 8–12 weeks. At higher arsenic doses, they observed extensive architectural disruption, loss of proximal tubular brush borders, vacuolation, cloudy swelling, and multiple haemorrhagic foci with mononuclear infiltration, which are consistent with the gross enlargement, interstitial haemorrhage, and tubular necrosis documented in our Group C at 12 weeks.[28] Similarly, Shangloo et al. noted dose-dependent renal pathology including disrupted architecture, altered periglomerular space, eosinophilic casts, and mononuclear cell infiltration, while controls retained normal renal architecture.[19] These lesions align closely with our observations of progressive glomerular changes in Group B and the advanced tubular and interstitial pathology in Group C. The consistency across studies reinforces the reliability of our results and highlights the predictable, dose-dependent trajectory of arsenic-induced renal injury.

Conclusion

The present study demonstrated a clear time- and dose-dependent pattern of hepatic and renal injury following chronic arsenic exposure. Control animals consistently maintained normal gross and microscopic architecture, validating the specificity of arsenic-induced lesions in exposed groups. In the liver, early changes were limited to focal inflammatory cell aggregates and central venous congestion, which progressively evolved into venous dilatation, chronic inflammatory infiltrates, and ultimately ballooning degeneration of hepatocytes in higher-dose animals. Similarly, the kidneys displayed a sequential injury pattern, beginning with vascular congestion and interstitial haemorrhage, advancing to glomerular shrinkage and Bowman's space widening, and culminating in tubular necrosis, interstitial haemorrhage, and fibrosis. Gross alterations were absent in early stages but became evident by twelve weeks, particularly in the high-dose group, with hepatic nodularity, discoloration, and renal enlargement with haemorrhagic patches.

Limitations: This study has several limitations. First, the small sample size (n=2 per group per timepoint) limits statistical power and generalizability. Second, actual arsenic intake could not be precisely determined as water consumption was not monitored. Third, the study relied on qualitative histopathological assessment without quantitative morphometry. Fourth, biochemical markers of hepatic and renal function were not measured, which would have provided functional correlates to the structural changes observed. Future studies should address these limitations and incorporate serum biochemistry and oxidative stress markers

..

REFERENCE

1. Sodhi KK, Kumar M, Agrawal PK, Singh DK. Perspectives on arsenic toxicity, carcinogenicity and its systemic remediation strategies. Environmental Technology & Innovation. 2019 Nov 1;16:100462.
2. Hu K, Islam MA, Parvez F, Bhattacharya P, Khan KM. Chronic exposure of arsenic among children in Asia: A current opinion based on epidemiological evidence. Current opinion in environmental science & health. 2024 Jun 1;39:100558.
3. Naujokas MF, Anderson B, Ahsan H, Aposhian HV, Graziano JH, Thompson C, Suk WA. The broad scope of health effects from chronic arsenic exposure: update on a worldwide public health problem. Environ Health Perspect. 2013 Mar;121(3):295-302. doi: 10.1289/ehp.1205875. Epub 2013 Jan 3. PMID: 23458756; PMCID: PMC3621177.
4. Abuawad A, Bozack AK, Saxena R, Gamble MV. Nutrition, one-carbon metabolism and arsenic methylation. Toxicology. 2021 Jun 15;457:152803. doi: 10.1016/j.tox.2021.152803. Epub 2021 Apr 24. PMID: 33905762; PMCID: PMC8349595.
5. Prakash C, Soni M, Kumar V. Mitochondrial oxidative stress and dysfunction in arsenic neurotoxicity: A review. J Appl Toxicol. 2016 Feb;36(2):179-88. doi: 10.1002/jat.3256. Epub 2015 Oct 29. PMID: 26510484.
6. LiverTox: Clinical and Research Information on Drug-Induced Liver Injury [Internet]. Bethesda (MD): National Institute of Diabetes and Digestive and Kidney Diseases; 2012-. Arsenic. [Updated 2017 Jul 25].
7. Ghatak S, Biswas A, Dhali GK, Chowdhury A, Boyer JL, Santra A. Oxidative stress and hepatic stellate cell activation are key events in arsenic induced liver fibrosis in mice. Toxicol Appl Pharmacol. 2011 Feb 15;251(1):59-69. doi: 10.1016/j.taap.2010.11.016. Epub 2010 Dec 4. PMID: 21134390; PMCID: PMC3745774.
8. Rana MN, Tangpong J, Rahman MM. Toxicodynamics of Lead, Cadmium, Mercury and Arsenic- induced kidney toxicity and treatment strategy: A mini review. Toxicol Rep. 2018 May 26;5:704-713. doi: 10.1016/j.toxrep.2018.05.012. PMID: 29992094; PMCID: PMC6035907.
9. Robles-Osorio ML, Sabath-Silva E, Sabath E. Arsenic-mediated nephrotoxicity. Renal failure. 2015 Apr 21;37(4):542-7.
10. Onan E, Ulu S, Güngör Ö. Heavy metals and kidney. Turk J Nephrol. Published online April 18, 2024. doi:10.5152/ turkjnephrol.2024.22497
11. Markowski VP, Currie D, Reeve EA, Thompson D, Wise JP Sr. Tissue-specific and dose-related accumulation of arsenic in mouse offspring following maternal consumption of arsenic-contaminated water. Basic Clin Pharmacol Toxicol. 2011 May;108(5):326-32. doi: 10.1111/j.1742-7843.2010.00660.x. Epub 2011 Jan 10. PMID: 21205216.
12. States JC, Barchowsky A, Cartwright IL, Reichard JF, Futscher BW, Lantz RC. Arsenic toxicology: translating between experimental models and human pathology. Environ Health Perspect. 2011 Oct;119(10):1356-63. doi: 10.1289/ehp.1103441. Epub 2011 Jun 17. PMID: 21684831; PMCID: PMC3230447.
13. Ramadan O, Abuamara T, Taha R, Awad M, Mohammed M, Omar N, Fayyad R, Darwish A, Eltantawy W, Babiker M, Elsharkawy S. Alleviation of the arsenic induced hepatotoxicity in rats by ginger or omega-3: a histological and biochemical study. Bioactive Compounds in Health and Disease-Online ISSN: 2574-0334; Print ISSN: 2769-2426. 2024 Apr 29;7(4):221-32.
14. Li J, Guo C, Liu Y, Han B, Lv Z, Jiang H, Li S, Zhang Z. Chronic arsenic exposure-provoked biotoxicity involved in liver-microbiota-gut axis disruption in chickens based on multi-omics technologies. J Adv Res. 2025 Jan;67:373-386. doi: 10.1016/j.jare.2024.01.019. Epub 2024 Jan 17. PMID: 38237767; PMCID: PMC11725159.
15. Santra A, Maiti A, Das S, Lahiri S, Charkaborty SK, Mazumder DN. Hepatic damage caused by chronic arsenic toxicity in experimental animals. J Toxicol Clin Toxicol. 2000;38(4):395-405. doi: 10.1081/clt-100100949. PMID: 10930056.
16. Rana MN, Tangpong J, Rahman MM. Toxicodynamics of Lead, Cadmium, Mercury and Arsenic- induced kidney toxicity and treatment strategy: A mini review. Toxicol Rep. 2018 May 26;5:704-713. doi: 10.1016/j.toxrep.2018.05.012. PMID: 29992094; PMCID: PMC6035907.
17. Noman AS, Dilruba S, Mohanto NC, Rahman L, Khatun Z, Riad W, Al Mamun A, Alam S, Aktar S, Chowdhury S, Saud ZA, Rahman Z, Hossain K, Haque A. Arsenic-induced Histological Alterations in Various Organs of Mice. J Cytol Histol. 2015 May;6(3):323. doi: 10.4172/2157-7099.1000323. Epub 2015 Apr 24. PMID: 26740907; PMCID: PMC4698904.
18. TOXICOLOGICAL PROFILE FOR ARSENIC. Atlanta (GA): Agency for Toxic Substances and Disease Registry (US); 2007 Aug. Available from: https://www.ncbi.nlm.nih.gov/books/NBK591633/

19. Shangloo P, Gupte B. Syed M. Histopathological Effect of Arsenic in Drinking Water on Liver and Kidney of Albino Rat: A Light Microscopic Study. International Journal of Scientific Research in Dental and Medical Sciences, 2021; 3(4): 166-170. doi: 10.30485/ijsrdms.2021.313575.1213
20. Ibrahim IK. Histological and histochemical study of effects of arsenic on the liver of adult male rabbits. The Egyptian Journal of Hospital Medicine. 2007 Oct 1;29(1):664-71.
21. Bhattacharya A, Dhar P, Mehra RD. Preliminary morphological and biochemical changes in rat liver following postnatal exposure to sodium arsenite. Anat Cell Biol. 2012 Dec;45(4):229-40. doi: 10.5115/acb.2012.45.4.229. Epub 2012 Dec 14. PMID: 23301191; PMCID: PMC3531587.
22. Ghatak S, Biswas A, Dhali GK, Chowdhury A, Boyer JL, Santra A. Oxidative stress and hepatic stellate cell activation are key events in arsenic induced liver fibrosis in mice. Toxicol Appl Pharmacol. 2011 Feb 15;251(1):59-69. doi: 10.1016/j.taap.2010.11.016. Epub 2010 Dec 4. PMID: 21134390; PMCID: PMC3745774.
23. Wen J, Li A, Wang Z, Guo X, Zhang G, Litzow MR, Liu Q. Hepatotoxicity induced by arsenic trioxide: clinical features, mechanisms, preventive and potential therapeutic strategies. Front Pharmacol. 2025 Feb 20;16:1536388. doi: 10.3389/fphar.2025.1536388. PMID: 40051569; PMCID: PMC11882591.
24. Li YY, Zheng TL, Xiao SY, Wang P, Yang WJ, Jiang LL, Chen LL, Sha JC, Jin Y, Chen SD, Byrne CD. Hepatocytic ballooning in non-alcoholic steatohepatitis: Dilemmas and future directions. Liver International. 2023 Jun;43(6):1170-82.
25. Parola M, Pinzani M. Liver fibrosis in NAFLD/NASH: from pathophysiology towards diagnostic and therapeutic strategies. Molecular aspects of medicine. 2024 Feb 1;95:101231.
26. Ferzand R, Gadahi JA, Saleha S, Ali Q. Histological and haematological disturbance caused by arsenic toxicity in mice model. Pakistan journal of biological sciences: PJBS. 2008 Jun 1;11(11):1405-13.
27. Roy S, Bhattacharya S. Arsenic-induced histopathology and synthesis of stress proteins in liver and kidney of Channa punctatus. Ecotoxicol Environ Saf. 2006 Oct;65(2):218-29. doi: 10.1016/j.ecoenv.2005.07.005. Epub 2005 Sep 16. PMID: 16150489.
28. Gupte B, Gupta S, Gupta V, et al. Histopathological effects of arsenic on kidneys of albino rats. International Journal of Emerging Technologies and Innovative Research. Vol.7, Issue 9, page no.1026-1034, September-2020, Available: http://www.jetir.org/papers/JETIR2009139.pdf

.